IEEE Access
Multidisciplinary | Rapid Review | Open Access Journal

Received December 3, 2018, accepted December 10, 2018, date of publication December 14, 2018,
date of current version January 11, 2019.

Digital Object Identifier 10.1109/ACCESS.2018.2886880

Friction Damper-Based Passive Vibration Control Assessment for Seismically-Excited Buildings Through Comparison With Active Control: A Case Study

ERCAN ATAM
[1]Independent Researcher, Reşitpaşa Mahallesi, Katar Caddesi, Teknokent ARI 1 Sitesi, 34467 Istanbul, Turkey
[2]Adjunct Faculty Member, Department of Mechatronics Engineering, Bahçeşehir University, 34349 Istanbul, Turkey

e-mail: ercan.atam@eng.bau.edu.tr

ABSTRACT In this paper, (i) we present a novel approach for easily developing mechanical models of buildings integrated with friction dampers to simplify their numerical simulation, and (ii) using the developed approach, friction damper-based passive control and then mass driver-based robust active vibration control strategies are applied on a seismically excited, three-story building simulation model, and the results are compared to assess the vibration attenuation level achieved by the passive control approach. The simulation results reveal that displacement and acceleration response reductions in active control are, in general, better than those in passive control but the difference is not that big. These findings, hence, encourage strongly the use of friction damper-based passive vibration control mechanisms as strong alternatives to active control methods in structural protection against earthquakes.

INDEX TERMS Smart buildings, earthquakes, friction dampers, passive control, robust control.

I. INTRODUCTION

Earthquakes are one of the most devastating disasters encountered in many countries, especially in Turkey. For such countries, seismic protection measures and technologies are important to minimize structural damage. Such a cost-effective measure is the integration of friction dampers (FDs) into buildings. FDs have started to be used in civil engineering structures in the early 1970s as passive structural control mechanisms [1], [3]. Since then, FDs became attractive structural elements for the suppression of vibrational effects due to wind loads [4]–[6], earthquake excitations [7]–[17], and other dynamic loads [18]. A friction damper system consists of a combination of a bracing frame and an energy absorbing mechanism using friction pads installed on the braced frame. They are designed to have moving parts which will slide over each other, and hence dissipate energy through friction during a strong excitation. Many kinds of friction dampers and installation configurations are available. Figure 1 shows a Sumitomo-type friction damper [1] and chevron-type installation configuration [2], which is the combination considered in this paper.

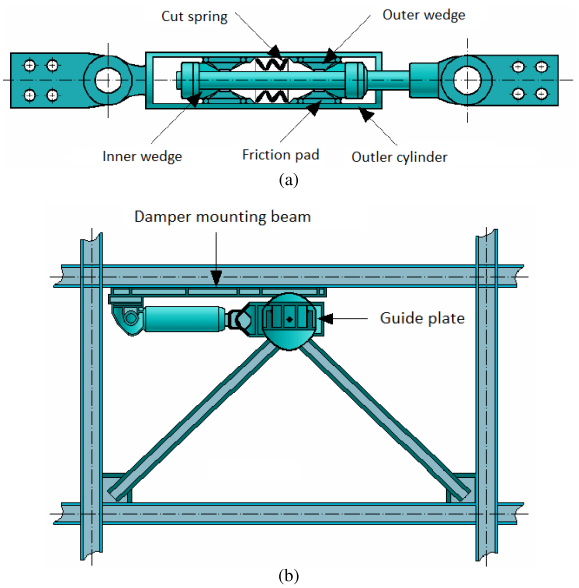

FIGURE 1. (a) Sumitomo-type friction damper [1], (b) its installation [2].

FDs with a constant friction force have a threshold value for the friction force. Depending on this value, sliding or sticking condition between the damper and main structure holds. The differential equations governing the system are coupled, and the number of these equations continuously changes depending on the sliding-sticking modes

TABLE 1. Pros and cons of FDs used in passive control of seismically excited buildings.

Pros	Cons
• Energy dissipation capacity of FDs is high. • FDs have a large rectangular hysteretic loop with negligible deterioration over many cycles of reversal [36]. • Compared to viscous dampers, the performance of FDs does not depend on temperature and velocity. • Behaviour of FDs is not seriously affected by the frequency and amplitude content of seismic excitation [9]. • FDs have a controllable friction force (through presentation of a normal force) [9]. • FDs are not affected by fatigue effects [9]. • In passive control design, no FD model information is used in the controller design. Hence, FD-based passive control is easy to design compared to semi-active or active control design. • In terms of cost considerations, FD-based passive control is cheaper compared to semi-active or active control. • FD systems are easy to install and replace.	• The energy absorbing capacity of FDs may deteriorate when their surface wears under strong earthquakes over many years. • Since the dynamics of FD-integrated buildings is highly nonlinear due to sliding-sticking alternations, simulation of FD-integrated buildings is not easy. • Sliding-sticking modes in FD-integrated buildings can introduce high frequencies into the building displacement and acceleration responses. • Deterministic optimal distribution of FDs is almost impossible to due dependency of sliding-sticking modes on the seismic input. As a result, only a stochastic optimal distribution can be determined. • Performance of FDs may be very suboptimal if a good FD distribution is not chosen. • In FD-based passive control, the energy dissipated per cycle is only proportional to maximum displacement instead of square of displacement as in the case of viscous dampers. This aspect is crucial in case of sudden pulses and more strong seismic inputs than expected [9]. • Durability of FDs is a parameter of concern due to high sensitivity of friction force to the condition of sliding surfaces which wear with time under strong earthquakes. • Due to the used bracing mechanism for installation of FDs, the building stiffness can increase considerably.

between the structure and the friction dampers. In sticking mode, they move together, and due to bracing the stiffness of the main structure increases which, in turn, may result in a decrease in system response. On the other hand, due to friction forces in the sliding case, a reduction in system response is achieved. The main difficulty in the analysis/design of such systems is that their behavior is highly non-linear and numerical simulation of their response is difficult. In the case of non-linear multi-degree freedom systems involving static friction, classical methods of vibration analysis fail since the number of degrees of freedom is not fixed. Table 1 lists the advantages and disadvantages of FDs used in seismic upgrade of buildings.

To overcome the drawbacks of constant friction force FDs, FDs with variable friction force have also been developed [19]–[21]. In such FDs, the level of friction force changes adaptively with structure's response. However, their cost is higher than the cost of constant friction force FDs.

As alternatives to passive structural control to improve the system performance, semi-active [22]–[31] and active control systems, especially using mass drivers [32]–[34], were developed considerably in the literature in the last decades. The main distinguishing difference between (semi-) active and passive control is the fact that (semi-) active control requires external power to operate, which may not be available during a strong seismic excitation, and hence (semi-) active control raises questions about both its reliability and practicality [35]. However, it should be noted semi-active devices can operate on batteries, so if this option is chosen, then the power outage during natural catastrophe is not the case in semi-active control.

The second disadvantage of active control for earthquake-resistant buildings is the typically large amount of required supply power, especially for tall buildings. On the other hand, active control has the advantage of feedback in the algorithm. The passive control systems do not have the above two cons of the active control but they may have the problem of inferior performance compared to active control.

In this paper, the focus is on two issues regarding passive and active control of seismically excited buildings, which are the contributions of the paper. First, we present a method to easily develop mechanical models of multi-story buildings equipped with FDs, which in turn simplifies their numerical simulation. The method is based on mechanical modeling and derivation of an equivalent viscous damping structure for the modal damping. This developed method results in a simple, easy-to-visualize computer-aided simulation model for systems with FDs. Next, using the developed method, the performance of the passive control approach using FDs with a constant friction force is compared to a robust active control method to see the performance level of the passive approach. In literature, there exist both types of control methods for seismically excited buildings, but there is no case study (to the best of our knowledge) which compares their performance to assess the performance level of constant

friction force FDs with respect to an active control method. Here, we perform such a study to close this gap which is our second contribution.

II. FULL DAMPING COUPLING-BASED MECHANICAL MODELLING APPROACH

Dynamic simulation of buildings with constant friction force FDs is hard, especially for large-scale multi-story buildings with tens of FDs, due to the sliding-sticking nature of FDs (and, hence the continuously changing degrees of freedom of the system). Simulation of such systems requires specially developed numerical codes. The objective of this section is to present a method which develops mechanical models for such systems, which, in turn, can easily be constructed and simulated in multi-body mechanical systems simulation tools, such as SimMechanics [37], Dymola [38], ADAMS [39]. The combination of the presented method with the use of such a tool will save considerable time and effort for simulation of large-scale multi-story buildings with tens of FDs.

Modeling of buildings with FDs is carried out in two steps. First, a mechanical model of the system is constructed and then updated using the idea of *full damping coupling* (the meaning and reasons of using full damping coupling will be clear later). Then, a SimMechanics [37] model of the final mechanical model is constructed and simulated. The reason behind using mechanical models is simply their easy visualization characteristics.

In general, modeling of multi-story buildings is based on shear-building idealization and lumped masses at floor levels. Consider a three-story building where a FD is incorporated at each floor. Each floor is a one-bay frame, and it is assumed that the structure has a symmetrical plan. The structure with FDs and its mechanical model are shown in Figure 2. The total degrees of freedom (DOF) of the system will change between three and six.

The mechanical model in Figure 2(b) is based on shear-building idealization. Now consider Figure 2(b) without FDs. The equations of motion involve mass, damping (structural), and stiffness matrices. The form of these matrices for a three-story building under shear-building assumption without FDs are

$$M = \begin{bmatrix} m_1 & 0 & 0 \\ 0 & m_2 & 0 \\ 0 & 0 & m_3 \end{bmatrix}, \quad K = \begin{bmatrix} k_1 + k_2 & -k_2 & 0 \\ -k_2 & k_2 + k_3 & -k_3 \\ 0 & -k_3 & k_3 \end{bmatrix},$$

$$C = \begin{bmatrix} c_1 + c_2 & -c_2 & 0 \\ -c_2 & c_2 + c_3 & -c_3 \\ 0 & -c_3 & c_3 \end{bmatrix}.$$

The calculation of mass is straightforward and the stiffness matrix is determined using the direct stiffness method from structural components of the building. In contrast, the damping coefficients c_1, c_2 and c_3 in Figure 2(b) are not known, and therefore this mechanical model cannot be simulated in its present form. The damping matric C cannot be evaluated from structural elements. To cope with this problem, modal damping ratios are assumed, and based on these ratios, the

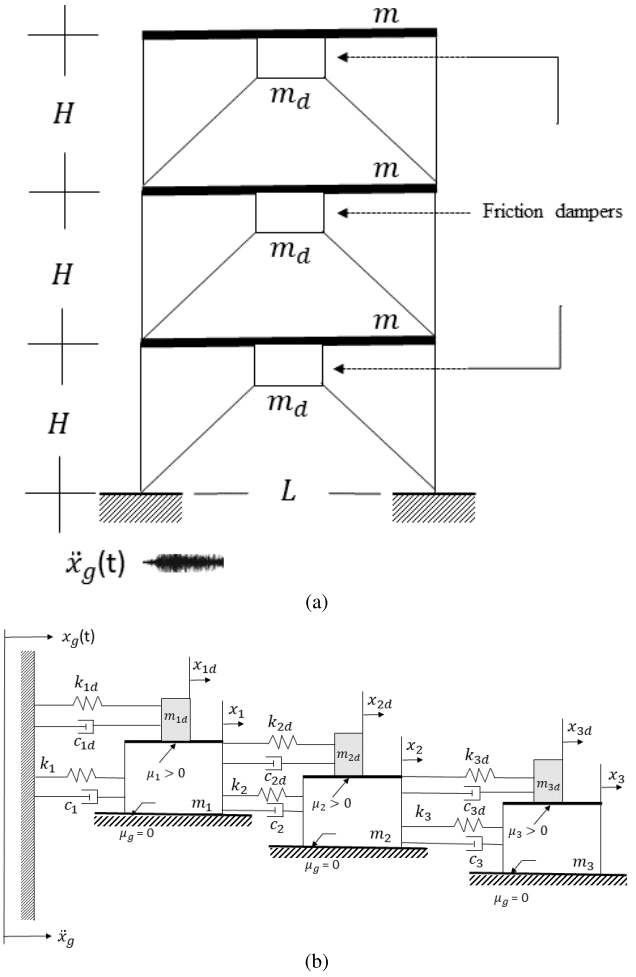

FIGURE 2. (a) A three-story building with FDs and (b) its mechanical model.

modal damping matrix of the structure is determined. This is a symmetric matrix and has the form

$$C_{\text{mdm}} = \begin{bmatrix} a & -b & -c \\ -b & d & -e \\ -c & -e & f \end{bmatrix}. \tag{1}$$

where the subscript "mdm" means the modal damping matrix. As seen, the form of the classical damping matrix C_{mdm} is different from that of the damping matrix of shear-building idealization, C. For the simulation of system response, C is replaced with C_{mdm}. For a mechanical model-based representation and simulation, this requires the modification of the corresponding mechanical models since they were constructed also under the assumption of shear-building idealization. Now, the question is how we will modify the mechanical model in Figure 2(b) to include the modal damping. The answer is as follows. The modal damping matrix C_{mdm} is a full matrix by which we mean its all entries may be different than zero. This suggests a mechanical model where *we must include a viscous damping coupling between each mass and between each mass and ground*. The mechanical model in Figure 3 illustrates this idea, and is an updated

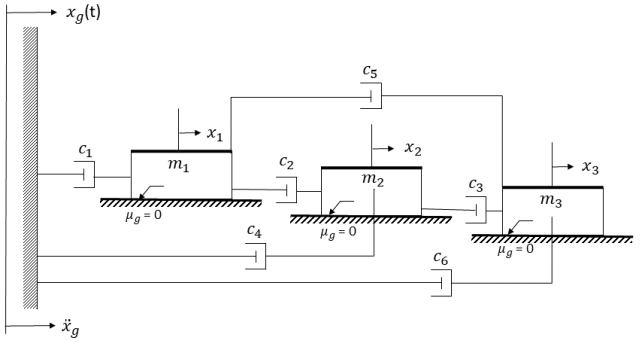

FIGURE 3. Updated mechanical model of a three-story building without stiffness and friction dampers.

version of the mechanical model in Figure 2(b) with ignore of stiffness and FDs.

The equations of motion of the system in Figure 3 are

$$m_1\ddot{x}_1 + (c_1 + c_2 + c_5)\dot{x}_1 - c_2\dot{x}_2 - c_5\dot{x}_3 = -m_1\ddot{x}_g, \quad (2a)$$
$$m_2\ddot{x}_2 + (c_2 + c_3 + c_4)\dot{x}_2 - c_2\dot{x}_1 - c_3\dot{x}_3 = -m_2\ddot{x}_g, \quad (2b)$$
$$m_3\ddot{x}_3 + (c_3 + c_5 + c_6)\dot{x}_3 - c_3\dot{x}_2 - c_5\dot{x}_1 = -m_3\ddot{x}_g. \quad (2c)$$

From this set of equations, an equivalent viscous damping matrix (equivalent to the modal damping matrix) is determined to be

$$C_{\text{evdm}} = \begin{bmatrix} c_1 + c_2 + c_5 & -c_2 & -c_5 \\ -c_2 & c_2 + c_3 + c_4 & -c_3 \\ -c_5 & -c_3 & c_3 + c_5 + c_6 \end{bmatrix}, \quad (3)$$

where the subscript ''evdm'' means equivalent viscous damping matrix. A comparison of (3) and (1) yields

$$c_1 = a - b - c, \quad c_2 = b, \; c_3 = e$$
$$c_4 = d - b - e, \quad c_5 = c, \; c_6 = f - e - c. \quad (4)$$

In summary, once we formed the modal damping matrix, the viscous damping coefficients $c_1, \cdots, c_6$ in the equivalent viscous damping matrix C_{evdm} are found using the equations in (4). Note that the mechanical model in Figure 3 is a virtual mechanical model, and hence the damping coefficients $c_1, \cdots, c_6$ have no physical meaning. The lateral stiffness of the chevron bracing on which a FD is installed is calculated later in the paper by (6). In the next section, we will consider a case study illustrating the presented idea.

III. CASE STUDY

The case study we chose is a symmetric, three-story building which is a four-bay planar frame in the x-direction and three-bay planar frame in the y-direction as shown in Figure 4. Table 2 includes the dimensions of columns for floors 1, 2 and 3, respectively. Other properties are given as follows: (i) All beam cross sections are 50×25 cm; (ii) Each floor thickness is assumed to be 0.12 m with density 25 kN/m^3; (iii) Self weight per length for outside walls is taken 12.5 kN/m; (iv) Self weight per length for inside walls is taken as 7 kN/m; (v) Self

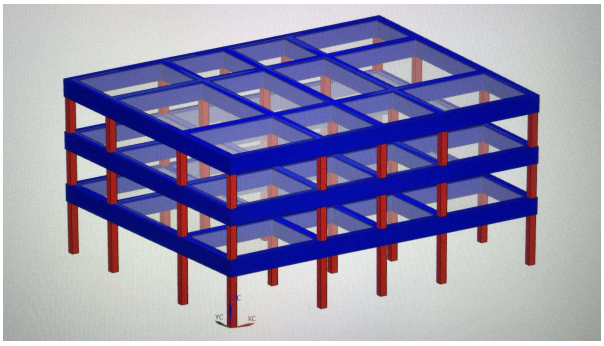

(a)

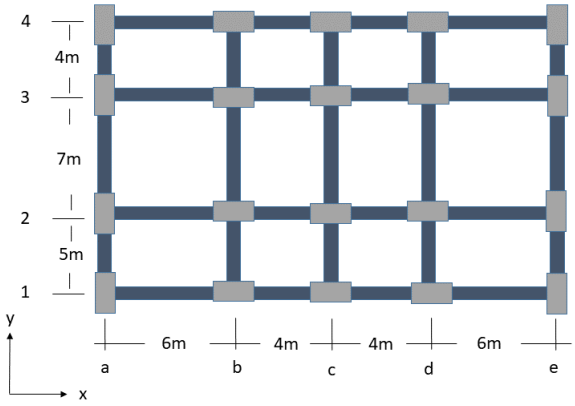

(b)

FIGURE 4. Example building: (a) plan view of the building studied for passive control-based and active control-based seismic response upgrade, (b) 2D top view of the building.

TABLE 2. Column dimensions (in cm) for first, second and third floors.

First floor	dx	dy
a_1, e_1, a_4, e_4	30	30
a_2, a_3, e_2, e_3	25	35
$b_1, c_1, d_1, b_4, c_4, d_4$	40	25
$b_2, c_2, d_2, e_2, b_3, c_3, d_3, e_3$	40	25
Second and third floors	dx	dy
a_1, e_1, a_4, e_4	30	30
a_2, a_3, e_2, e_3	25	30
$b_1, c_1, d_1, b_4, c_4, d_4$	30	25
$b_2, c_2, d_2, e_2, b_3, c_3, d_3, e_3$	35	25

weight per volume for beams and columns including fine works is taken as 30 kN/m^3; (vi) The live load per area is 3 kN/m^2.

Using the geometric properties and the above data, the mass of each floor is found to be 3802.60 kg. The modulus of elasticity of the reinforced concrete is determined from Turkish Standards [40] as

$$E = 3250\sqrt{0.85 \times cs_{BS20}} + 1400 \quad (5)$$

using BS20-type reinforced concrete for older structures to be upgraded seismically. Here, cs_{BS20} is the cylindrical strength of BS20 type concrete, 20 N/mm^2 with material safety factor of 15 percent. The 28-day strength, E, is calculated to be 28500 N/mm^2. The frame is modeled as a moment resisting

shear type frame. The objective is to improve the seismic response of this structure using a fixed number of friction dampers. As ground acceleration, we choose the north-south component of İzmit-Turkey, August 17, 1999 ground acceleration. The peak value of the ground acceleration is 171.172 mg. Here, only the x-direction motion is considered. Friction dampers are mounted on chevron bracings, and each damper-bracing combination is placed in the x-direction spaces between two columns. The maximum number of friction dampers to be used is 48 since for each of the three floors, we have $4\times4 = 16$ spaces. The lateral stiffness of the chevron bracing, ignoring compression resistance, is determined from the following expression (see Eq. (3.3) in [9, Ch. 3]):

$$k' = \frac{2E_bAL^2}{(4H^2 + L^2)^{3/2}}, \tag{6}$$

where E_b is Young's modulus for the bracing material, A is the cross-section area of bracing, and L, H are span width and height, respectively. Since the x-direction span widths are either 6 m or 4m, we have two different stiffness values, $k_1' = 32.67 \times 10^6$ N/m and $k_2' = 23.66 \times 10^6$ N/m. In simulations, spans of 6 m width are considered first and then 4 m width spans are used. The cross-section of the chevron bracing is type IPE120. The threshold of friction force between the main structure and the friction dampers is taken to be 45 kN. Data related to each friction damper are summarized in Table 3.

TABLE 3. Friction damper parameters and their values.

E_b (N/m)	$2.1x10^{11}$
A (cm^2)	13.2
L_1 (m)	6
L_2 (m)	4
H (m)	3
m_d (kg)	40
k_1' (N/m)	$32.67x10^6$
k_2' (N/m)	$23.66x10^6$

The stiffness matrix is calculated using the code number technique and direct stiffness method [41], [42]. The classical damping matrix is determined using Caughey method [43], taking a modal damping ratio of 0.05 for each mode. The natural frequencies of the building are calculated to be 9.63 rad/s, 26.4 rad/s and 36.58 rad/s. Since the modal damping ratios are very small, the damped natural frequencies are nearly equal to these values.

The updated final mechanical model of the structure for the case of using all friction dampers is shown in Figure 5. Each damper is connected with a spring (which is the lateral stiffness of the chevron bracing on which damper is mounted) either to the wall or to the big masses and for the sake of simplicity, we have shown this for only one damper on each floor mass. In Figure 5, μ is used to denote the friction force coefficient. The displacement response of the structure under the considered seismic excitation is found for the following cases: (i) structure without any friction damper, (ii) structure with all friction dampers, (iii) structure with all combinations of using 16 friction dampers.

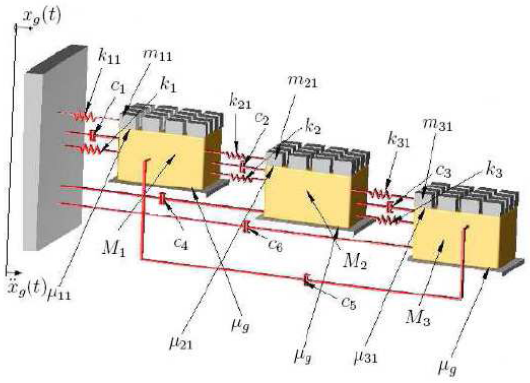

FIGURE 5. Mechanical model of the case study building with integrated FDs.

For the last case, all possible combinations are simulated and then the data are sorted in ascending order with respect to the sum of maximum story drifts. From this sorted data, the best case (optimal) and worst case distributions of dampers are determined corresponding to the considered seismic excitation. Table 4 shows displacement responses and FD distributions corresponding to the following cases: (i) structure with no friction damper case or bare structure case (bare), (ii) best case distribution of 16 FDs (best), (iii) worst case distribution of 16 FDs (worst), and (iv) structure with all 48 dampers case (full). In this table, n_i denotes the number of friction dampers used at i-th floor, u_i is the maximum displacement of the i-th floor with respect to ground, d_i is the maximum story drift and $\sum d_i$ is the sum of maximum story drifts.

Finally, in the reduction of seismic response, the following criteria must be satisfied for the structure to remain in its elastic range when it deforms [44]

$$\frac{(d_i)_{max}}{h_i} \leq 0.0035, \tag{7}$$

where $(d_i)_{max}$ is the maximum story drift and h_i is the story height. This condition is satisfied by best and full case distributions. From the results in Table 4, we see that the best distribution of the 16 dampers between floors is 8-5-3 and the performance of this distribution of 16-dampers is very close to the use of all 48 dampers. This clearly shows that the full integration of a building with FDs may be very unnecessary. Figure 6 shows the floor displacements relative to ground for the best and the worst cases, all compared with the response of bare structure. In all graphs, *cs* means the controlled structure with friction dampers.

In addition to comparison of displacement responses, we need to compare also the acceleration responses because high floor accelerations can result in sudden jerky motions which can damage equipment in the building and reduce occupant comfort during long duration ground motions [45], [46]. Passive control floor acceleration responses for the

TABLE 4. Bare, best, worst, full damper case distributions and maximum displacements.

NS	n_1	n_2	n_3	$u_1(cm)$	$u_2(cm)$	$u_3(cm)$	$d_1(cm)$	$d_2(cm)$	$d_3(cm)$	$\sum d_i$
bare	0	0	0	1.41	3.21	4.26	1.41	1.80	1.07	4.28
best	8	5	3	0.53	1.05	1.42	0.53	0.69	0.48	1.70
worst	1	0	15	1.61	3.51	4.20	1.61	2.08	0.81	4.50
full	16	16	16	0.55	0.94	1.22	0.55	0.47	0.41	1.43

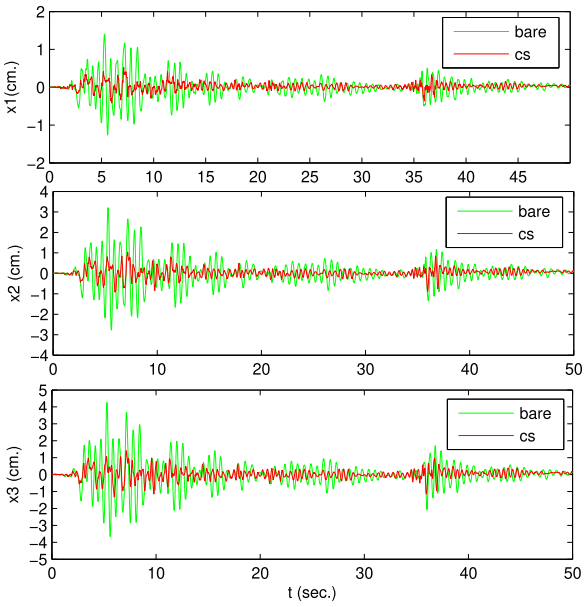

(a)

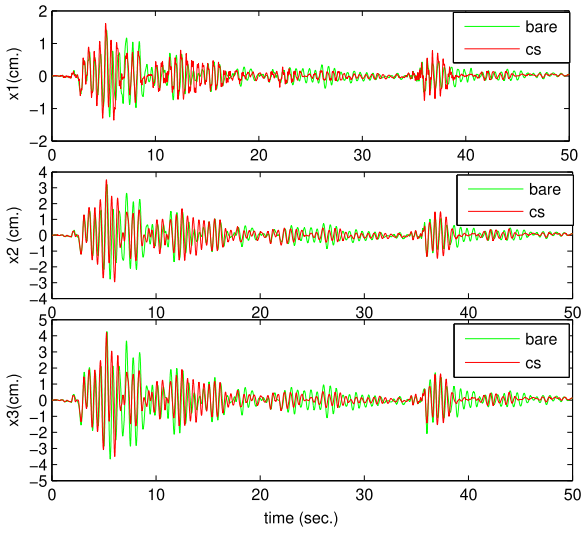

(b)

FIGURE 6. Passive control floor displacement responses (with comparison to the bare case): (a) the best case, (b) the worst case.

best case (building with 8-5-3 FD distribution) are compared with floor acceleration responses of the bare case in Figure 7 and in Table 5. From the comparisons we see that acceleration response reduction performance of passive control is also significant, in terms of both reduction of peak value of acceleration and reduction of average value of absolute acceleration over the considered time period.

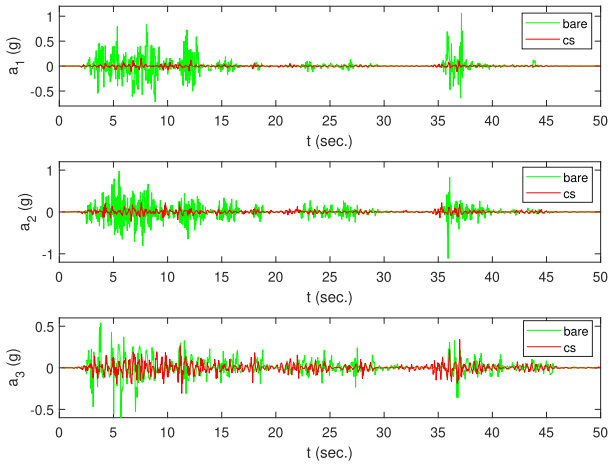

FIGURE 7. Passive control floor acceleration responses (with comparison to the bare case) for the best case. The accelerations are specified in terms of acceleration of gravity, *g*.

Remarks:

- Thanks to the presented full damping coupling method, Figure 5 was easily developed, which was then constructed in SimMechanics [37] to simulate the system. This way, the simulation of buildings with FDs under ground accelerations becomes extremely easy.
- For buildings with FDs, the optimal distribution of a fixed number FDs for a given *arbitrary* ground acceleration seems an interesting research problem. However, a deterministic solution cannot be found for such systems since the sliding-sticking mode (hence, the total energy dissipation level) depends on the ground acceleration. However, a statistical approach is possible: under all possible combinations of the fixed number of FDs and hundreds of ground accelerations, and after an extensive number of simulations, a statistical result can be given on the best possible distribution of the fixed number of FDs. Such a study will be considered in future.

IV. ACTIVE CONTROL

Active Mass Driver (AMD) system is the most commonly used method of active control in seismic protection of buildings and we will also use that one. The AMD system consists of a mass whose motion is controlled by the actuator. The AMD system is usually put on the roof of the buildings so that control force is just applied to the top floor but in this study we will use an AMD system for each floor as shown in Figure 8.

One of the most important issues to consider in active control is the robustness of the control algorithm. Robust control

TABLE 5. Bare (building without FDs) and best case floor acceleration response comparisons under the considered seismic excitation. Accelerations are specified in terms of acceleration of gravity, *g*. Maximum value of absolute acceleration is shortened as "max. abs. a" and average value of absolute acceleration is shortened as "avg. abs. a".

	Bare case max. abs. a	FD-integrated best case max. abs. a	Bare case avg. abs. a	FD-integrated best case avg. abs.a
First floor	1.0622	0.1592	0.0795	0.0105
Second floor	1.1076	0.2390	0.1023	0.0252
Third floor	0.5991	0.3400	0.0649	0.0344

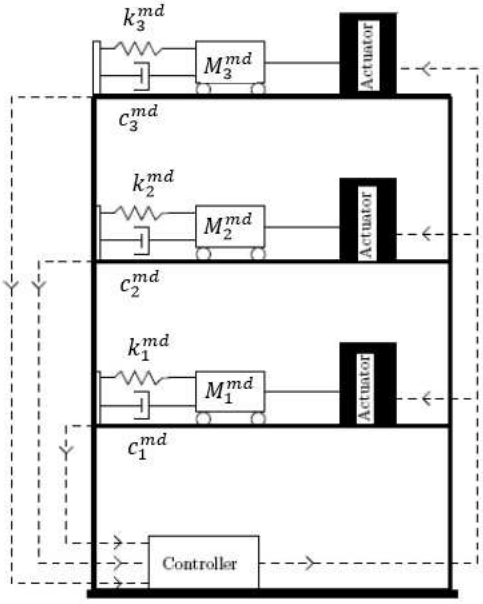

FIGURE 8. Active mass driver system. In the figure, "md" means mass driver.

focuses on the performance and stability of the system in the presence of uncertainty. Here, we will assume parametric uncertainties in the stiffness and damping matrices, which are unavoidable in the modeling of multi-story buildings. Nominal mass matrix will be used because in general the mass of a multi-story building can be calculated accurately.

Next, a robust controller will be designed for the three-story example model building considered in passive control part. Let M^0, C^0, K^0 be the nominal building matrices and M, C, K be the corresponding ones including uncertainty. Since no uncertainty in mass is assumed, we have $M = M^0$. To begin with, we derive the unifying framework for robust control shown in Figure 9.

The nominal mass, damping and stiffness matrices of the building were

$$M^0 = \begin{bmatrix} m_1^0 & 0 & 0 \\ 0 & m_2^0 & 0 \\ 0 & 0 & m_3^0 \end{bmatrix},$$

$$C^0 = \begin{bmatrix} c_1^0 + c_2^0 + c_5^0 & -c_2^0 & -c_5^0 \\ -c_2^0 & c_2^0 + c_3^0 + c_4^0 & -c_3^0 \\ -c_5^0 & -c_3^0 & c_3^0 + c_5^0 + c_6^0 \end{bmatrix},$$

$$K^0 = \begin{bmatrix} k_1^0 + k_2^0 & -k_2^0 & 0 \\ -k_2^0 & k_2^0 + k_3^0 & -k_3^0 \\ 0 & -k_3^0 & k_3^0 \end{bmatrix}.$$

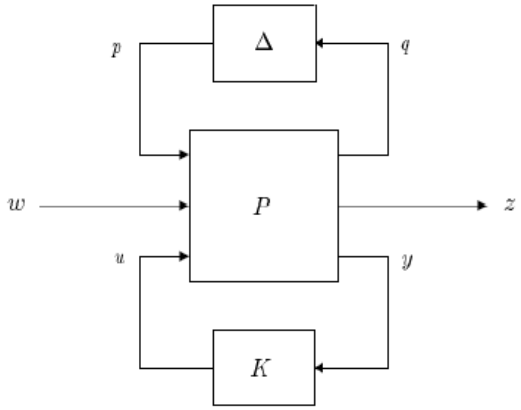

FIGURE 9. Robust control framework.

The nominal and uncertain parameters can be written as

$$\begin{aligned} m_1 &= = m_1^0, \quad m_2 = m_2^0, \\ m_3 &= m_3^0, \quad c_1 = c_1^0 + w_{c_1} c_1^0 \delta_{c_1}, \\ c_2 &= c_2^0 + w_{c_2} c_2^0 \delta_{c_2}, \quad c_3 = c_3^0 + w_{c_3} c_3^0 \delta_{c_3}, \\ c_4 &= c_4^0 + w_{c_4} c_4^0 \delta_{c_4}, \quad c_5 = c_5^0 + w_{c_5} c_5^0 \delta_{c_5}, \\ c_6 &= c_6^0 + w_{c_6} c_6^0 \delta_{c_6}, \quad k_1 = k_1^0 + w_{k_1} k_1^0 \delta_{k_1}, \\ k_2 &= k_2^0 + w_{k_2} k_2^0 \delta_{k_2}, \quad k_3 = k_3^0 + w_{k_3} k_3^0 \delta_{k_3}, \end{aligned}$$

where w_{c_i} and w_{k_j} are weightings for damping and stiffness coefficients and they represent the degree of uncertainty in each quantity, $\delta_{c_i}, \delta_{k_i} \in [-1, 1]$ are the normalized uncertainties. The uncertain damping matrix C can be decomposed as

$$C = C^0 + W_{C_1} \triangle_C W_{C_2}, \tag{8}$$

where

$$W_{C_1} = \begin{bmatrix} w_{c_1} c_1^0 & w_{c_2} c_2^0 & 0 & 0 & 0 & w_{c_6} c_6^0 \\ 0 & -w_{c_2} c_2^0 & w_{c_3} c_3^0 & w_{c_4} c_4^0 & 0 & 0 \\ 0 & 0 & -w_{c_3} c_3^0 & 0 & w_{c_5} c_5^0 & -w_{c_6} c_6^0 \end{bmatrix},$$

$$\triangle_C = \begin{bmatrix} \delta_{c_1} & 0 & 0 & 0 & 0 & 0 \\ 0 & \delta_{c_2} & 0 & 0 & 0 & 0 \\ 0 & 0 & \delta_{c_3} & 0 & 0 & 0 \\ 0 & 0 & 0 & \delta_{c_4} & 0 & 0 \\ 0 & 0 & 0 & 0 & \delta_{c_5} & 0 \\ 0 & 0 & 0 & 0 & 0 & \delta_{c_6} \end{bmatrix},$$

$$W_{C_2} = \begin{bmatrix} 1 & 0 & 0 \\ 1 & -1 & 0 \\ 0 & 1 & -1 \\ 0 & 1 & 0 \\ 0 & 0 & 1 \\ 1 & 0 & -1 \end{bmatrix}.$$

Similarly, the uncertain stiffness matrix K is written as

$$K = K^0 + W_{K_1} \triangle_K W_{K_2} \tag{9}$$

where

$$W_{K_1} = \begin{bmatrix} w_{k_1}k_1^0 & w_{k_2}k_2^0 & 0 \\ 0 & -w_{k_2}k_2^0 & w_{k_3}k_3^0 \\ 0 & 0 & -w_{k_3}k_3^0 \end{bmatrix},$$
$$\triangle_K = \begin{bmatrix} \delta_{k_1} & 0 & 0 \\ 0 & \delta_{k_2} & 0 \\ 0 & 0 & \delta_{k_3} \end{bmatrix}, W_{K_2} = \begin{bmatrix} 1 & 0 & 0 \\ 1 & -1 & 0 \\ 0 & 1 & -1 \end{bmatrix}.$$

The equation of motion of the three-story building using the mass, damping and stiffness matrices can be written as

$$M^0\ddot{\zeta} + \left(C^0 + W_{C_1}\triangle_C W_{C_2}\right)\dot{\zeta} + \left(K^0 + W_{K_1}\triangle_K W_{K_2}\right)\zeta = d + u \tag{10}$$

where d is the disturbance force associated with ground acceleration and u is the control input force. The displacement vector ζ is relative to ground. Letting $x = [x_1\ x_2]^T = [\zeta\ \dot{\zeta}]^T$, equation (10) can be written as

$$\dot{x}_2 = -(M^0)^{-1}[C^0x_2 + K^0x_1 + W_{C_1}\triangle_C W_{C_2}x_2 + W_{K_1}\triangle_K W_{K_2}x_1 - d - u]. \tag{11}$$

Now make the following substitutions

$$q_c = W_{C_2}x_2, \quad p_c = \triangle_C W_{C_2}x_2 = \triangle_C q_c,$$
$$q_k = W_{K_2}x_1, \quad p_k = \triangle_K W_{K_2}x_1 = \triangle_K q_k.$$

Using these substitutions, Equation (11) can be written as

$$\dot{x}_2 = -(M^0)^{-1}\left(C^0x_2 + K^0x_1 + W_{C_1}p_c + W_{K_1}p_k - d - u\right). \tag{12}$$

Then, the equation of motion can be put into the following form

$$\dot{x} = Ax + B_pp + B_dd + B_uu \tag{13}$$

with

$$A = \begin{bmatrix} 0 & I \\ -(M^0)^{-1}K^0 & -(M^0)^{-1}C^0 \end{bmatrix},$$
$$B_p = \begin{bmatrix} 0 & I \\ -(M^0)^{-1}W_{C_1} & -(M^0)^{-1}W_{K_1} \end{bmatrix}, \quad p = \begin{bmatrix} p_c \\ p_k \end{bmatrix},$$
$$B_d = B_u = \begin{bmatrix} 0 \\ (M^0)^{-1} \end{bmatrix}.$$

In the unifying framework of Figure 9, w represents all disturbances including sensor noise n in the measured signals. Taking this fact into consideration, disturbance signal w consists of the force due to seismic excitation and sensor noise. Namely, $w = [d\ n]^T$. Then, Equation (13) can be rewritten as

$$\dot{x} = Ax + B_pp + B_ww + B_uu, \tag{14}$$

where $B_w = [B_d\ 0]^T$. Remember that $q_c = W_{C2}x_2$, $q_k = W_{K2}x_1$. From these two relations, we get

$$q = C_qx + D_{qp}p + D_{qw}w + D_{qu}u, \tag{15}$$

where

$$q = \begin{bmatrix} q_c \\ q_k \end{bmatrix}, \quad C_q = \begin{bmatrix} 0 & W_{C_2} \\ W_{K_2} & 0 \end{bmatrix}, \ D_{qp} = D_{qw} = D_{qu} = 0.$$

For the output to be controlled or regulated, we choose $z = [x_1\ W_uu]^T$ where x_1 is the displacement vector containing floor displacements. W_u is the control input weighting matrix. The choice of this weighting matrix is important because it is directly related to the magnitude of the control force to be produced. If its entries are increased, the associated control force decreases, and if decreased, the control force increases. Therefore, by playing with that matrix, the appropriate control force is determined. Using $z = [x_1\ W_uu]^T$, we can write the controlled output equation as

$$z = C_zx + D_{zp}p + D_{zw}w + D_{zu}u, \tag{16}$$

where

$$C_z = \begin{bmatrix} I & 0 \\ 0 & 0 \end{bmatrix}, \quad D_{zp} = D_{zw} = 0, D_{zu} = \begin{bmatrix} 0 \\ W_u \end{bmatrix}.$$

Finally, x_1 is chosen for the measured output, and hence the input to the controller is

$$y = x_1 + n. \tag{17}$$

Similarly, Equation 17 is rewritten as

$$y = C_yx + D_{yp}p + D_{yw}w + D_{yu}u \tag{18}$$

where $C_y = C_z$, $D_{yp} = D_{yu} = 0$, $D_{yw} = [0\ W_n]^T$ and W_n is the noise weighting matrix. Equations (14), (15), (16) and (18) are the state-space equations of the robust control framework of the problem and are summarized below.

$$\begin{aligned} \dot{x} &= Ax + B_pp + B_ww + B_uu, \\ q &= C_qx + D_{qp}p + D_{qw}w + D_{qu}u, \\ z &= C_zx + D_{zp}p + D_{zw}w + D_{zu}u, \\ y &= C_yx + D_{yp}p + D_{yw}w + D_{yu}u. \end{aligned}$$

A robust controller is designed using these system matrices. Ten percent uncertainty in each damping and stiffness coefficients is assumed so that all damping and stiffness wightings are 0.1 and nominal mass matrix is used. After some trial and error, the optimal control input and noise weights to minimize the maximum sum of story drifts were chosen as

$$W_u = 3 \times 10^{-5}I_3, \quad W_n = 5 \times 10^{-6}I_3.$$

The mass, damping and stiffness coefficients of each of three AMDs are take to be 20 kg, 5×10^2 Ns/m and 20×10^3 N/m, respectively. D-K iteration gave at the second iteration a 12^{th} order controller with achieved *gamma* and *mu* value of 0.164 and 0.163 respectively. From the *gamma* and *mu*

TABLE 6. Actively controlled structure displacement quantities.

	u_1 (cm)	u_2 (cm)	u_3 (cm)	d_1 (cm)	d_2 (cm)	d_3 (cm)	$\sum d_i$ (cm)
puc	0.46	0.87	1.06	0.46	0.43	0.21	1.1
muc	0.52	0.96	1.15	0.52	0.46	0.22	1.2

values obtained from the D-K iteration, it is seen that they are much less than one, and therefore robust stability and performance objectives are well achieved. Figure 10(a) shows the floor displacements relative to ground using the active control system and taking the damping and stiffness coefficients to be 1.1 times their nominal values and call that case "plus uncertainty case" (puc). Figure 10(b) shows the same quantities using the active control system and taking the damping and stiffness coefficients to be 0.9 times their nominal values. This case is called "minus uncertainty case" (muc). In all figures, "cs" denotes the actively controlled structure.

The maximum displacements of first, second and third floors relative to ground, maximum story drifts and their sum are shown in Table 6. From these results, we see that active control achieves a good displacement response reduction.

From comparison of results in Table 4 and Table 6, we see that the best-case distribution of 16 FDs (8-5-3) gives a performance, in terms of displacement response reduction, close to performance of active control cases.

Next, floor acceleration responses of active control cases (both plus and minus uncertainty cases) are compared with bare case floor acceleration responses in Figure 11 and Table 7. As we see, the performance of active control in terms of acceleration response reduction is also very satisfactory.

If we compare acceleration response reduction ability of the best case of passive control to that of the active control using Table 5 and Table 7, we see that acceleration response reductions in active control cases are in general better (except, for the colored cells in Table 7, for which a possible reason is the conservativeness of the active robust controller) but the differences with passive control are not so big.

To sum up, response reduction performance of passive control both in terms of displacement and acceleration response reduction is close to performance of active control, signifying the power of seismic vibration control using a FD-based passive approach.

Remarks:

- It is crucial that the active controller be designed based on a robust control approach since uncertainty in the stiffness and damping matrices is unavoidable. For example, in practical applications the behavior of real buildings may deviate to some extent from that of idealized shear buildings.
- Here, the comparison between the FD-based passive control and active control results may be thought of unfair since the active control results are based on a robust controller. However, this is not the case since the passive control design is not a model-based approach (*i.e.*, no model information was used). Moreover, when we compared the passive control results with an H_∞ controller designed using nominal system matrices, the results of passive control were close again.
- When we used four scaled versions of the considered ground excitation as input (with scaling coefficients = 1.5, 2, 2.5, 3 to take into account different peak ground accelerations) and tested the control approaches, the performances of both active and passive control were good, and the results were again close to each other. These

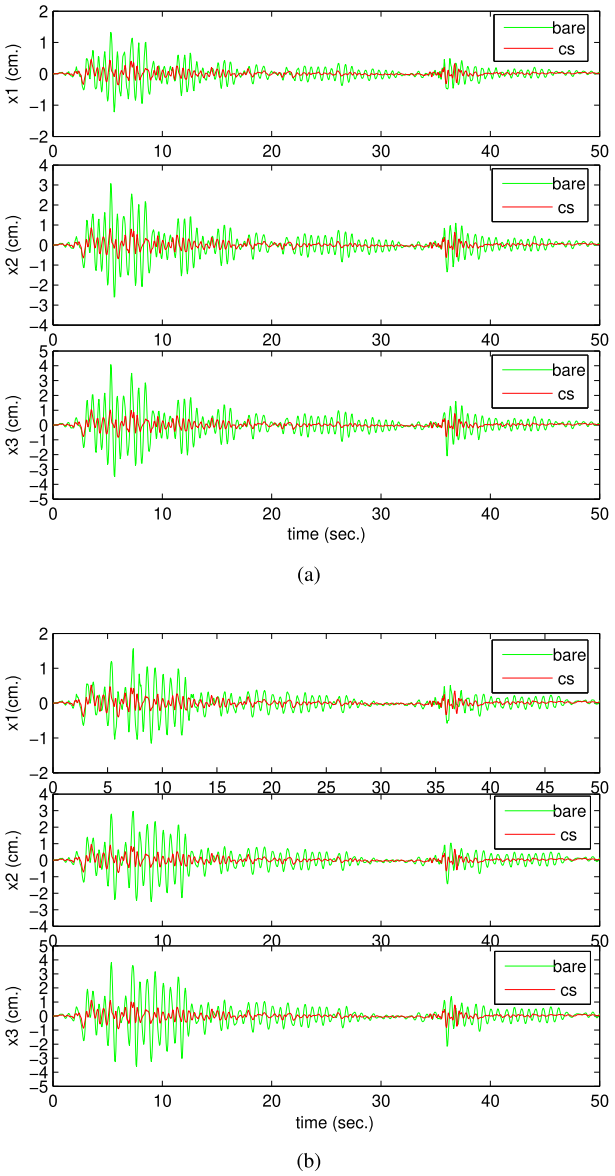

FIGURE 10. Active seismic control floor displacements (with comparison to bare case) under uncertainties in the system matrices: (a) puc, (b) muc.

TABLE 7. Bare (building without FDs) and active control cases floor acceleration response comparisons under the considered seismic excitation. Accelerations are specified in terms of acceleration of gravity, *g*. Maximum value of absolute acceleration is shortened as "max. abs. a" and average value of absolute acceleration is shortened as "avg. abs. a". The colored cells show the quantities which are higher than the corresponding values in Table 5 of the best case of passive control.

"puc case"	Bare case max. abs. a	Active control "puc" case max. abs. a	Bare case avg. abs. a	Active control "puc" case avg. abs.a
First floor	1.0622	0.1379	0.0795	0.0111
Second floor	1.1076	0.1499	0.1023	0.0172
Third floor	0.5991	0.4176	0.0649	0.0224
"muc case"	Bare case max. abs. a	Active control "muc" case max. abs. a	Bare case avg. abs. a	Active control "muc" case avg. abs.a
First floor	1.0622	0.0795	0.0795	0.0091
Second floor	1.1076	0.3926	0.1023	0.0178
Third floor	0.5991	0.2960	0.0649	0.0204

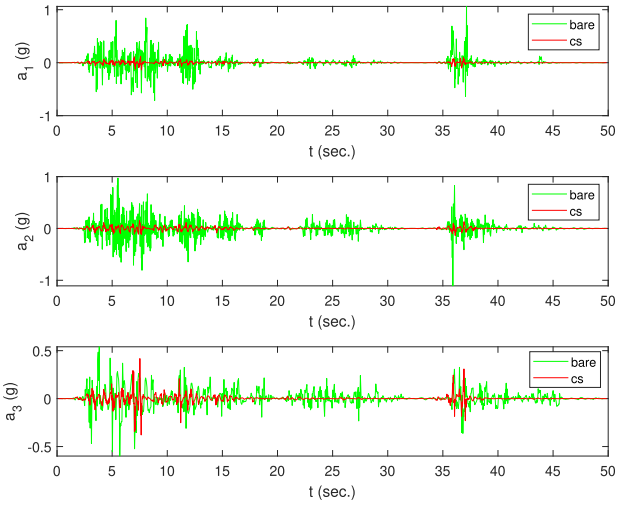

(a)

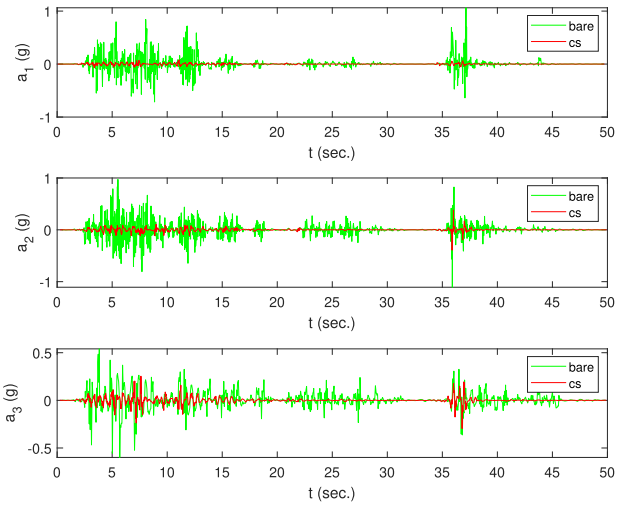

(b)

FIGURE 11. Active seismic control floor acceleration responses (with comparison to bare case) under uncertainties in the system matrices: (a) puc, (b) muc. The accelerations are specified in terms of acceleration of gravity, *g*.

results were not presented here since the scaled ground accelerations did not correspond to recorded real ground accelerations. These simulations were performed to only gain confidence on the findings of this study.

- The active control results do not depend on the mass, damping and stiffness values in the driver since in the approach followed, the driver dynamics were decoupled from the building dynamics, and it was assumed that the driver system is able to produce the control input $u = k^{md}\nu + c^{md}\dot{\nu}$ where ν is the relative displacement vector of the drivers with respect to building stories. As a result, it is not the case to have better active control results by the optimal tuning of the driver parameters M^{md}, k^{md} and c^{md}. However, the selection of M^{md}, k^{md} and c^{md} should be done so that ν does not exceed half of the floor lengths assuming that the initial position of each AMD is the center of each floor and that the actuator force $F_a = k^{md}\nu + c^{md}\dot{\nu} + M^{md}\ddot{\nu}$ is producible by the actuators at floors. These are the only constraints on driver parameters.

V. CONCLUSIONS AND FUTURE WORK

In this paper, first we presented a simple method based on the idea of full damping coupling to develop mechanical models for multi-story buildings integrated with friction dampers to simplify their numerical simulation. The developed method is valuable in case of large-scale multi-story buildings with tens of friction dampers. The developed mechanical models can be constructed easily in an appropriate multi-body simulation tool to simulate multi-story buildings with friction dampers. This saves a lot of effort and time compared to development of special numerical codes for simulation of such complicated systems where DOF of the system may change continuously.

Next, using the developed method, the FD-based passive seismic control approach was compared with a mass driver-based active robust control approach to assess its performance, which is not available in the open literature to our best knowledge. The results revealed that passive control achieves a good performance and hence motivates the integration of FD devices to have earthquake-resistant buildings. Although it was shown that the use of FDs results in a considerable seismic response reduction, it was observed that the distribution of the dampers is of great importance because some distributions may cause a seismic response increase instead of decrease. Moreover, it was observed that integration of a building with a small number of FDs gives a seismic response reduction close to the one with a full integration.

The main finding of this paper is that the low-cost solution friction damper integration into buildings against earthquake loads gives a protection level close to using an active control solution based on a mass driver system. Moreover, it should be taken into account that compared to FD-based passive control, mass driver-based active control has the disadvantage of the possibility of the cut of electricity power during earthquakes (unless supported with an electric generator) which causes stopping of its functioning.

As future work, (i) regarding FD-based passive control, a statistical approach can be developed to determine optimal distribution of a fixed number of FDs between floors using an extensive number of simulations under a set of ground excitations; (ii) regarding active control, an explicit model predictive control method can be developed where soft constraints on both floor displacements and accelerations can be imposed.

REFERENCES

[1] A. S. Pall, C. Marsh, and P. Fazio, "Friction joints for seismic control of large panel structures," *J. Prestressed Concrete Inst.*, vol. 25, no. 6, pp. 38–61, 1980.

[2] E. N. Farsangi and A. Adnan, "Seismic performance evaluation of various passive damping systems in high and medium-rise buildings with hybrid structural system," *Gazi Univ. J. Sci.*, vol. 25, no. 3, pp. 721–735, 2012.

[3] M. C. Constantinou, T. T. Soong, and G. F. Dargush, "Passive energy dissipation systems for structural design and retrofit," Multidiscipl. Center Earthquake Eng. Res., USA, Tech. Rep. 1, 1998.

[4] V. B. Patil and R. S. Jangid, "Double friction dampers for wind excited benchmark building," *Int. J. Appl. Sci. Eng.*, vol. 7, no. 2, pp. 95–114, 2009.

[5] F. Mazza and A. Vulcano, "Control of the along-wind response of steel framed buildings by using viscoelastic or friction dampers," *Wind Struct.*, vol. 10, no. 3, pp. 233–247, 2007.

[6] W. L. Qu, Z. H. Chen, and Y.-L. Xu, "Dynamic analysis of wind-excited truss tower with friction dampers," *Comput. Struct.*, vol. 79, no. 32, pp. 2817–2831, 2001.

[7] I. Takewaki, *Building Control with Passive Dampers: Optimal Performance-based Design for Earthquakes*, 1st ed. Hoboken, NJ, USA: Wiley, 2009.

[8] A. Pall, S. Vezina, P. Proulx, and R. Pall, "Friction-dampers for seismic control of Canadian space agency headquarters," *Earthquake Spectra*, vol. 9, no. 3, pp. 547–557, 1993.

[9] C Cháidez, "Contribution to the assessment of the efficiency of friction dissipators for seismic protection of buildings," Ph.D. dissertation, Dept. Eng. Terreny, Cartografica Geofisica, Politecnic Univ. Catalunya, Barcelona, Spain, 2003.

[10] A. K. Agrawal and M. Amjadian, "Seismic component devices," in *Innovative Bridge Design Handbook*. London, U.K.: Butterworths-Heinemann, 2015, pp. 531–553.

[11] I. H. Mualla and B. Belev, "Performance of steel frames with a new friction damper device under earthquake excitation," *Eng. Struct.*, vol. 24, no. 3, pp. 365–371, 2002.

[12] C.-G. Cho and M. Kwon, "Development and modeling of a frictional wall damper and its applications in reinforced concrete frame structures," *Earthquake Eng. Struct. Dyn.*, vol. 33, no. 7, pp. 821–838, 2004.

[13] A. V. Bhaskararao and R. S. Jangid, "Seismic analysis of structures connected with friction dampers," *Eng. Struct.*, vol. 28, no. 5, pp. 690–703, 2006.

[14] S.-H. Lee, J.-H. Park, S.-K. Lee, and K.-W. Min, "Allocation and slip load of friction dampers for a seismically excited building structure based on storey shear force distribution," *Eng. Struct.*, vol. 30, no. 4, pp. 930–940, 2008.

[15] M. Mirtaheri, A. P. Zandi, S. S. Samadi, and H. R. Samani, "Numerical and experimental study of hysteretic behavior of cylindrical friction dampers," *Eng. Struct.*, vol. 33, no. 12, pp. 3647–3656, 2011.

[16] M. Saitoh, "An external rotary friction device for displacement mitigation in base isolation systems," *Struct. Control Health Monit.*, vol. 21, no. 2, pp. 173–188, 2014.

[17] S. T. de la Cruza, F. López-Almansa, and S. Oller, "Numerical simulation of the seismic behavior of building structures equipped with friction energy dissipators," *Comput. Struct.*, vol. 85, no. 12, pp. 30–42, 2007.

[18] A. Golafshani and A. Gholizad, "Friction damper for vibration control in offshore steel jacket platforms," *J. Construct. Steel Res.*, vol. 65, no. 1, pp. 180–187, 2009.

[19] S. Laflamme, D. Taylor, M. A. Maane, and J. J. Connor, "Modified friction device for control of large-scale systems," *Struct. Control Health Monit.*, vol. 19, no. 4, pp. 548–564, 2012.

[20] Y. L. Xu and C. L. Ng, "Seismic protection of a building complex using variable friction damper: Experimental investigation," *J. Eng. Mech.*, vol. 134, no. 8, pp. 637–649, 2008.

[21] H. Dai, Z. Huang, and W. Wang, "A new permanent magnetic friction damper device for passive energy dissipation," *Smart Mater. Struct.*, vol. 23, no. 10, p. 105016, 2014.

[22] J. N. Yang, J. C. Wu, and Z. Li, "Control of seismic-excited buildings using active variable stiffness systems," *Eng. Struct.*, vol. 18, no. 8, pp. 589–596, 1996.

[23] D. Marinova and V. Marinov, "Numerical design of optimal active control for seismically-excited building structures," in *Proc. 3rd Int. Conf. Numer. Anal. Appl.*, Rousse, Bulgaria, Jun./Jul. 2004, pp. 408–415.

[24] H. Yazici and R. Guclu, "Fuzzy logic control of a non-linear structural system against earthquake induced vibration," *J. Vib. Control*, vol. 13, no. 11, pp. 1535–1551, 2007.

[25] H. Ghaffarzadeh, E. A. Dehrod, and N. Talebian, "Semi-active fuzzy control for seismic response reduction of building frames using variable orifice dampers subjected to near-fault earthquakes," *J. Vib. Control*, vol. 19, no. 13, pp. 1980–1999, 2012.

[26] Y. Ikeda, "Active and semi-active control of buildings in Japan," *J. Jpn. Assoc. Earthquake Eng.*, vol. 4, no. 3, pp. 278–282, 2004.

[27] S. Pourzeynali and T. Mousanejad, "Optimization of semi-active control of seismically excited buildings using genetic algorithms," *Sci. Iranica. Trans. A, Civil Eng.*, vol. 17, no. 1, pp. 26–38, 2010.

[28] M. D. Symans and M. C. Constantinou, "Semi-active control systems for seismic protection of structures: A state-of-the-art review," *Eng. Struct.*, vol. 21, no. 6, pp. 469–487, 1999.

[29] W. L. He, A. K. Agrawal, and J. N. Yang, "Novel semiactive friction controller for linear structures against earthquakes," *J. Struct. Eng.*, vol. 129, no. 7, pp. 941–950, 2003.

[30] C. L. Ng and Y. L. Xu, "Semi-active control of a building complex with variable friction dampers," *Eng. Struct.*, vol. 29, no. 6, pp. 1205–1229, 2007.

[31] D. H. Zhao and H. N. Li, "Shaking table tests and analyses of semi-active fuzzy control for structural seismic reduction with a piezoelectric variable-friction damper," *Smart Mater. Struct.*, vol. 19, no. 10, 2010, Art. no. 105031.

[32] T. Kobori, N. Koshika, N. Yamada, and Y. Ikeda, "Seismic-response-controlled structure with active mass driver system. Part 1: Design," *Earthquake Eng. Struct. Dyn.*, vol. 20, no. 2, pp. 133–149, 1991.

[33] M. Yamamoto, S. Aizawa, M. Higashino, and K. Toyama, "Practical applications of active mass dampers with hydraulic actuator," *Earthquake Eng. Struct. Dyn.*, vol. 30, no. 11, pp. 1697–1717, 2001.

[34] M. Yamamoto and T. Sone, "Behavior of active mass damper (AMD) installed in high-rise building during 2011 earthquake off Pacific coast of Tohoku and verification of regenerating system of AMD based on monitoring," *Struct. Control Health Monit.*, vol. 21, no. 4, pp. 634–647, 2014.

[35] T. S. Jeffrey, "Structural control using regenerative force actuation networks," Ph.D. dissertation, Dept. Civil Eng., California Inst. Technol., Pasadena, CA, USA, 2004.

[36] S. G. Nikam, S. K. Wagholikar, and G. R. Patil, "Seismic energy dissipation of a building using friction damper," *Int. J. Innov. Technol. Exploring Eng.*, vol. 3, no. 10, pp. 61–64, 2014.

[37] *MATLAB Simmechanics Toolbox*, MathWorks, Natick, MA, USA, 2015.

[38] (2016). *Dassault Systmes AB, Dymola*. [Online]. Available: http://www.claytex.com/products/dymola

[39] MSC Software Corp. (2018). (ADAMS). [Online]. Available: http://www.mscsoftware.com/product/adams

[40] *Specification for Structures to be Built in Disaster Areas, Part III*, Ministry Public Works Resettlement, Turkey, 1997.

[41] S. S. Tezcan, "Discussion of the simplified formulation of stiffness matrices," *J. Struct. Division*, vol. 89, pp. 445–449, 1963.

[42] A. Kassimali, *Matrix Analysis of Structures*, 2nd ed. Standford, CA, USA: Cengage Learning, 2011.

[43] A. K. Chopra, *Dynamics of Structures: Theory and Applications to Earthquake Engineering*, 4th ed. Upper Saddle River, NJ, USA: Prentice-Hall, 2011, p. 454.

[44] *Turkish Earthquake Code*, Ministry Public Works Resettlement, Turkey, 1998.

[45] P. Dupont, P. Kasturi, and A. Stokes, "Semi-active control of friction dampers," *J. Sound Vib.*, vol. 202, no. 2, pp. 203–218, 1997.

[46] M. Amjadian and A. K. Agrawal, "A passive electromagnetic eddy current friction damper (PEMECFD): Theoretical and analytical modeling," *Struct. Control Health Monit.*, vol. 24, no. 10, p. e1978, 2017.

ERCAN ATAM received the Ph.D. degree in mechanical engineering from Boğaziçi University, Istanbul, Turkey, in 2010. He was a Postdoctoral Researcher with LIMSI-CNRS, Paris, France, from 2010 to 2012, working on fluid flow control. From 2012 to 2015, he has been a Postdoctoral Researcher with KU Leuven, Belgium, where he was involved in control and optimization of energy-efficient buildings. Since 2016, he has been an Independent Researcher. His research interests include structural control, robust control, LPV control, MPC, optimization, and machine learning.